Phonon-mediated anisotropic superconductivity in the Y and Lu nickel borocarbides

P. Martínez-Samper,[1] H. Suderow,[1] S. Vieira,[1] J. P. Brison,[2] N. Luchier,[2] P. Lejay,[2] and P. C. Canfield[3]
[1]*Laboratorio de Bajas Temperaturas, Departamento de Física de la Materia Condensada, Instituto de Ciencia de Materiales Nicolás Cabrera, Facultad de Ciencias, Universidad Autónoma de Madrid, 28049 Madrid, Spain*
[2]*Centre des Recherches sur les Très Basses Températures, CNRS, BP 166, 38042 Grenoble, Cedex 9, France*
[3]*Ames Laboratory and Department of Physics and Astronomy, Iowa State University, Ames, Iowa 50011*
(Received 6 June 2002; revised manuscript received 2 December 2002; published 29 January 2003)

We present scanning tunneling spectroscopy and microscopy measurements at low temperatures in the borocarbide materials $R\mathrm{Ni_2B_2C}$ ($R=$Y, Lu). The characteristic strong-coupling structure due to the pairing interaction is unambiguously resolved in the superconducting density of states. It is located at the superconducting gap plus the energy corresponding to a phonon mode identified in previous neutron-scattering experiments. These measurements also show that this mode is coupled to the electrons through a highly anisotropic electron-phonon interaction originated by a nesting feature of the Fermi surface. Our experiments, from which we can extract a large electron-phonon coupling parameter λ (between 0.5 and 0.8), demonstrate that this anisotropic electron-phonon coupling has an essential contribution to the pairing interaction. The tunneling spectra show an anisotropic *s*-wave superconducting gap function.

DOI: 10.1103/PhysRevB.67.014526 PACS number(s): 74.20.Mn, 74.62.Dh, 74.70.Dd

I. INTRODUCTION

In most known superconductors the formation of Cooper pairs is based on an attractive interaction mediated by phonons. However, Cooper pairing driven by other Bosonic excitations has also attracted much attention due to its fundamental interest. Some of the proposed mechanisms have been used to interpret the superconducting behavior of different compounds discovered during the last decades. But clear microscopic information is very much needed in this field. The situation is especially puzzling in the borocarbide materials ($R\mathrm{Ni_2B_2C}$, $R=$Y, Lu, Tm, Er, Ho, Dy), where recent experiments have shown that the question about the pairing interaction, initially thought to be conventional electron-phonon coupling,[1–3] is far from being understood. These compounds show moderate critical temperatures [between 6 and 16.5 K (Refs. 4 and 5)] and very interesting phase diagrams where superconductivity coexists with antiferromagnetic order (when R is a magnetic rare earth, $R=$Tm, Er, Ho, Dy). The behaviors observed in the thermal conductivity,[6,7] photoemission spectroscopy,[8] specific heat,[9,10] microwave surface impedance,[9,11] and Raman-scattering[12] experiments of the nonmagnetic Y and Lu borocarbides (which also present the highest critical temperatures of 15.5 and 16.5 K, respectively) show that the superconducting gap is highly anisotropic. Indirectly, this could be related to an also anisotropic pairing interaction, but no experiment has given an indication of its nature.

On the other hand, Fermi surface nesting seems to be a general feature of the whole family of borocarbide materials. It produces Kohn anomalies and has directly been observed using angular correlation of electron-positron annihilation radiation in $\mathrm{YNi_2B_2C}$ and $\mathrm{LuNi_2B_2C}$.[13–15] Moreover, the antiferromagnetic ordering found in the borocarbides with a magnetic rare earth has a wave vector very close to the nesting vector $Q\approx(0.5,0,0)$ (Refs. 16 and 17) (in $R=$Er, Ho, and Dy; in Tm it appears in a magnetic-field phase). Nesting is generally considered to play against the formation of a phonon mediated superconducting state, as evidenced in other families of superconductors (e.g., in the dichalchogenides[18,19]). Here we present measurements of tunneling spectroscopy of the nonmagnetic $\mathrm{YNi_2B_2C}$ and $\mathrm{LuNi_2B_2C}$, which show that the highly anisotropic electron-phonon interaction produced by Fermi surface nesting drives the system to an also anisotropic superconducting state. We give insight into the nature of the pairing mechanism, the order parameter symmetry, and the gap anisotropy.

II. EXPERIMENT

Tunneling spectroscopy is in principle one of the most powerful experimental tools to investigate the anisotropy of the superconducting gap and to obtain information about the pairing mechanism.[20] We use the same scanning tunneling microscopy and spectroscopy (STM/STS) setup as in Ref. 21, where we studied the magnetic $\mathrm{TmNi_2B_2C}$, with an improved resolution allowing now measurements down to 0.5 K. We have also characterized other materials with the same setup (Al,[22] Pb, and $\mathrm{NbSe_2}$) and demonstrated that this is indeed the actual temperature of tip and sample and that we do not need any additional pair breaking parameter Γ[8] to explain our data. Previous works about the spectroscopy of borocarbides had a lower resolution in energy.[8,23–25] The sample is broken in air on the sample holder of the STM and cooled down immediately. The resulting surface presents the same topology as for the Tm borocarbide, which consists of inclined planes and bumps, typical of a conchoidal fracture, presenting no clear crystallographic orientation.[21] So it is crucial to characterize the superconducting behavior in well-differentiated regions of the sample. We use a home made *x-y* table that gives the possibility to change *in situ* the scanning window (of $1\times1\,\mu\mathrm{m}^2$) in an area of 2×2 mm^2. We measured three different samples (in three different cooldowns) of each compound. In the case of $\mathrm{LuNi_2B_2C}$, all of them were freshly broken pieces of the same single crystal grown by a flux technique described in Ref. 5. The $\mathrm{YNi_2B_2C}$

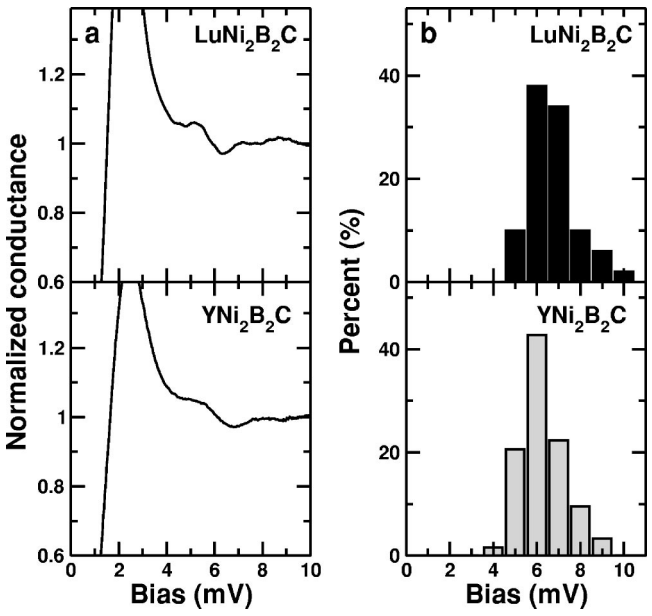

FIG. 1. (a) Tunneling conductance spectra (taken at 0.5 K and normalized to the conductance value at high bias voltage) where electron-phonon coupling features at high voltages clearly appear. (b) Histogram counting the number of times we find such a feature (within a sample of a hundred spectra), with the maximum value of the derivative of the conductance at the voltage reported on the *x* axis.

samples came from two different single crystals, one grown by the same flux technique and the other in an image furnace. The tunneling conditions were always very good, with high valued measured work functions of several eV.

III. RESULTS AND DISCUSSION

The tunneling differential conductance, $\sigma = dI/dV$, between a normal metal and a superconductor gives a direct (temperature smeared) measurement of the superconducting density of states. Therefore data show the eventual presence of very low-energy excitations within the superconducting gap 2Δ, and a high quasiparticle peak at voltages close to the gap. But if the measurement is sufficiently precise, one can also try to resolve tiny features at voltages corresponding to the sum of Δ and the characteristic energy of the Bosonic excitations leading to superconductivity, in order to obtain information about the nature of these excitations.[20,26,27] We could indeed observe these features in the tunneling conductance spectra for the Y and Lu borocarbides. In Fig. 1 we show a typical curve together with a histogram where the number of times that such features are observed is presented as a function of the bias voltage (their voltage position is determined from the maximum of the derivative of the conductance above the gap[20,26,27]). Most of them appear centered at a voltage between 6 and 7 mV. Subtracting the values of Δ, as estimated below, the maxima become centered between 4 and 5 mV. This is precisely the energy at which a high peak develops in neutron-scattering experiments due to a low-energy phonon mode.[13,14] From our data we can estimate the electron-phonon coupling constant $\lambda = 2\int d(\omega)\alpha^2 F(\omega)/\omega$, obtaining the electron-phonon spectral function, $\alpha^2 F(\omega)$, as in Ref. 28 (this leads to the same result as the conventional inversion procedure[20]). We get rather high values between 0.5 and 0.8 in both compounds. On the other hand, previous estimations using thermodynamic measurements, which take into account the Eliashberg function at all relevant phonon frequencies, but which do not directly specify the nature or spectral weight of each mode, have given values of λ between 0.75 and 1.2.[29,30] The fact that we find values of λ smaller but very close to the ones estimated with thermodynamic measurements means that the structures in the Eliashberg function associated with higher energy phonon modes[31,32] are more spread out in energy than the peak corresponding to the 4-mV phonon mode and fall below our experimental resolution. It also means that the low-energy phonon mode measured here is essential in the formation of superconducting correlations.

The most striking point, however, is that the phononic density of states at these energies results from a mode having a wave vector comparable to the nesting vector Q (0.5,0,0).[15,17] Neutron-scattering experiments show indeed pronounced Kohn anomalies,[13,14] where the nesting feature of the Fermi surface[15,17] leads to a significant softening, when decreasing temperature, of the low-lying transverse phonon branches at wave vectors close to (0.5,0,0). This behavior results in a strong and highly anisotropic electron-phonon coupling. Our experiment demonstrates that this anisotropic electron-phonon interaction, produced by Fermi surface nesting, leads to superconducting correlations, having an important contribution to the total electron-phonon coupling constant λ. Correspondingly, we can expect the superconducting gap to be also highly anisotropic.

Tunneling conductance measurements done with a STM give the superconducting density of states averaged over part (but not all) of the Fermi surface, depending on the relative position of the tip onto the sample.[33] In most cases we measure tunneling conductance curves as the ones shown in Fig. 2, where the conductance is zero below 0.8 mV and then increases up to a peak located at 2.6 mV in Lu and 2.3 mV in Y. These curves cannot be fitted by conventional BCS theory. The discrepancy with most simple BCS theory is not due to a lifetime smeared BCS density of states, which leads to a nonzero density of states at low energies, not observed in our data. The situation is clearly very different from the one found in the very similar borocarbide material $TmNi_2B_2C$,[21] where the spectra can be fitted by BCS theory. The form of the curves in Fig. 2 shows that the electrons contributing to the tunneling current at this precise location come from parts of the Fermi surface with a continuous distribution of values of the superconducting gap.[34,35] This reveals that the gap function must be anisotropic. Moreover, the spectra in $(Y,Lu)Ni_2B_2C$ remain with the same shape over regions much larger than the coherence length (usually dimensions about 200×200 nm^2 or bigger whereas $\xi\simeq7$ nm, Ref. 9), maintaining their overall form when we increase the temperature, and becoming completely flat at the bulk critical temperature. Similar observations have been made in the anisotropic superconductor $NbSe_2$,[34,35] where the spectra have, qualitatively, the same form.

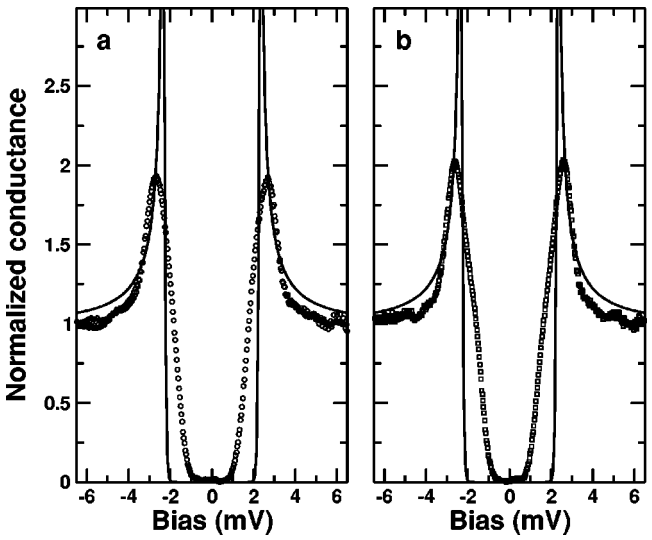

FIG. 2. Tunneling conductance spectra in the Lu (a) and Y (b) borocarbides at 0.5 K normalized to the conductance value at high bias voltage (tunneling resistance of 2 MΩ). The full lines are fits to conventional BCS theory ($\Delta = 2.3$ meV).

On the other hand, although the behavior shown in Fig. 2 appears most frequently on the surface, we can also find different topographical regions of similar sizes with very different spectra, as shown in Fig. 3. There is a clear correspondence between the topography and superconducting density of states on the surface of the samples.

In order to analyze this relationship, we compare in Fig. 4(a) the temperature dependence of Δ, as estimated from the voltage position of the maximum of $d\sigma/dV$, and in Fig. 4(b) the corresponding tunneling density of states at 0.5 K in three different locations of YNi_2B_2C (the same is observed in $LuNi_2B_2C$). This shows that the differences in the spectra found in diverse topographic regions (Fig. 3) are associated with smaller values of the superconducting gap and also a reduced critical temperature. Remarkably, the mean value of the superconducting gaps shown in Fig. 4(a) follows well the temperature dependence predicted by simple BCS theory (lines). What is more, the curves corresponding to a smaller critical temperature in Fig. 4(b) (top curve) approach much better an isotropic BCS *s*-wave behavior than those corresponding to the bulk T_c (bottom curve). This must be related

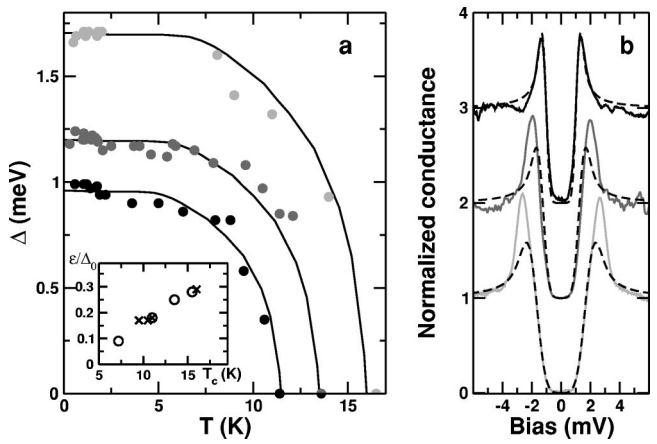

FIG. 4. (a) Temperature dependence of the mean value of the superconducting gap (points) in YNi_2B_2C. We take Δ as the voltage where $d\sigma(V)/dV$ is maximum. Lines give the temperature dependence of the superconducting gap expected in BCS theory. The inset represent the variation of ε/Δ_0 (see text) with T_c for YNi_2B_2C (circles) and $LuNi_2B_2C$ (crosses). (b) Spectra taken at 0.5 K for each temperature run [same color for the straight lines as points in (a), shifted for clarity]. Dashed lines are fits to the BCS theory with anisotropy (see text), where, from top to bottom, $\Delta_0 = 1.1$ mV and $\varepsilon = 0.2$ mV, $\Delta_0 = 1.3$ mV and $\varepsilon = 0.32$ mV, and $\Delta_0 = 1.8$ mV and $\varepsilon = 0.5$ mV.

to changes in the anisotropy as a function of the local T_c.

To obtain more quantitative information about this effect we have fitted the experiment to a modified BCS *s*-wave density of states assuming that the dispersion in the values of the superconducting gap can be modeled by a Gaussian distribution centered around Δ_0 with a width of ε. A similar approach has been previously used in the anisotropic superconductor $NbSe_2$.[35] The dashed lines in Fig. 4(b) give the best fit to this model. The agreement with the experiment is much better in regions with a smaller T_c, where ε decreases. The inset in Fig. 4(a) represents the dependence of the estimated anisotropy ε/Δ_0 as a function of the measured critical temperature in several topographical regions of the same samples. Note that these values do not give an indication of the whole distribution of values of the superconducting gap, as a given STM spectrum is a local measurement which probes only part of the Fermi surface.[33] Therefore our data

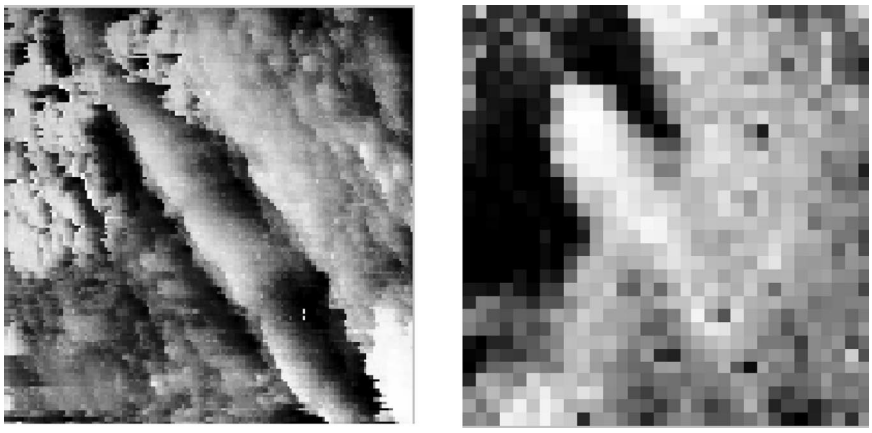

FIG. 3. Topographic (left) and STS (right) images at 0.5 K (YNi_2B_2C, 310×310 nm^2). The latter figure is indicative of the superconducting density of states as a function of the position of the tip on the surface.[21,25] The contrast is adjusted such that bright spots correspond to $\sigma(V)$ similar to Fig. 2(b), and dark spots to $\sigma(V)$ similar to the top curve in Fig. 4(b).

are in good agreement to previous macroscopic measurements.[6–12,42,43]

Anisotropic superconductivity is expected to be very sensitive to even nonmagnetic defects that reduce T_c and decrease the anisotropy.[36,37] Therefore, in an anisotropic superconductor, local measurements in topographically different positions on the surface can in principle show different forms of the superconducting gap and values of the local critical temperature, associated with the presence of defects lying near the surface or with an irregular topography.[38] Isotropic superconductors, by contrast, present BCS spectra and the bulk critical temperature over the whole surface.[21,22,39]

In $(Y,Lu)Ni_2B_2C$ we observe a gradual decrease of the local critical temperature down to about half its bulk value *and* of the anisotropy [inset of Fig. 4(a)] in different locations which also show a different topography (Fig. 3). Our measurements show a direct correlation between the local depression of T_c with a local change of the form of the gap. This also demonstrates that the superconducting gap must be highly anisotropic, and it provides an additional test of the nature of the order parameter in these materials. If the anisotropy is due to a *d*-wave order parameter, the defects tend to suppress superconductivity altogether and low-energy excitations appear, filling the density of states below the gap. If, however, the superconducting wave function is anisotropic *s* wave, the defects tend to suppress the anisotropy, leading to a more isotropic gap and a decreased critical temperature.[40,41] The curves plotted in Fig. 4(b), with no low-energy excitations, definitely imply that superconductivity in YNi_2B_2C and $LuNi_2B_2C$ is highly anisotropic but *s* wave.

Using the same experimental protocol, we find a completely different behavior in the chemically very similar magnetic $TmNi_2B_2C$ compound ($T_c = 11$ K), where BCS *s*-wave-like spectra without a significant anisotropy (and bulk critical temperature) are measured over the whole surface.[21] However, we can state that the surface is analogous in all three compounds, because the measured work function and the topographical images are similar. This could be interpreted as an indication that mechanisms inducing anisotropy in YNi_2B_2C and $LuNi_2B_2C$ are not operating in this borocarbide, or that the intrinsic magnetic disorder already smears out homogeneously the anisotropy.

IV. SUMMARY

In summary, we have studied the tunneling spectroscopy in the nonmagnetic borocarbides using high-resolution STM/STS. We have been able to characterize important microscopic aspects of the superconducting state, which is an anisotropic *s*-wave state, where a significant part of the electron-phonon coupling leading to superconducting correlations is also highly anisotropic and due to soft phonons. The demonstration of this interesting mechanism strengthens the hope for further discoveries in the area of new high-T_c superconducting materials.

ACKNOWLEDGMENT

We acknowledge discussions with Professor D. González, F. Guinea, A. I. Buzdin, J. Flouquet, and A. Levanyuk, and support from the ESF program VORTEX, from the MCyT (Spain; Grant No. MAT-2001-1281-C02-0), from FERLIN, and from the Comunidad Autónoma de Madrid (Spain). The Laboratorio de Bajas Temperaturas is associated to the ICMM of the CSIC. Ames Laboratory is operated for the U. S. Department of Energy by Iowa State University under Contract No. W-7405-Eng-82. This work was supported by the Director for Energy Research, Office of Basic Energy Sciences.

[1] L.F. Mattheiss, Phys. Rev. B **49**, 13 279 (1994).

[2] I.K. Yanson, V.V. Fisun, A.G.M. Jansen, P. Wyder, P.C. Canfield, B.K. Cho, C.V. Tomy, and D.McK. Paul, Phys. Rev. Lett. **78**, 935 (1997).

[3] K.O. Cheon, I.R. Fisher, and P.C. Canfield, Physica C **312**, 35 (1999).

[4] R.J. Cava *et al.* Nature (London) **367**, 146 (1994); R. Nagarajan, C. Mazumdar, Z. Hossain, S.K. Dhar, K.V. Gopalakrishnan, L.C. Gupta, C. Godart, B.D. Padalia, and R. Vijayaraghavan, Phys. Rev. Lett. **72**, 274 (1994).

[5] P.C. Canfield, P.L. Gammel, and D.J. Bishop, Phys. Today **51** (10), 40 (1998).

[6] E. Boaknin, R.W. Hill, C. Proust, C. Lupien, L. Taillefer, and P.C. Canfield, Phys. Rev. Lett. **87**, 237001 (2001).

[7] K. Izawa, K. Kamata, Y. Nakajima, Y. Matsuda, T. Watanabe, M. Nohara, H. Takagi, P. Thalmeier, and K. Maki, Phys. Rev. Lett. **89**, 137006 (2002).

[8] T. Yokoya, T. Kiss, T. Watanabe, S. Shin, M. Nohara, H. Takagi, and T. Oguchi, Phys. Rev. Lett. **85**, 4952 (2000).

[9] K. Izawa, A. Shibata, Y. Matsuda, Y. Kato, H. Takeya, K. Hirata, C.J. van der Beek, and M. Konczykowski, Phys. Rev. Lett. **86**, 1327 (2001).

[10] M. Nohara, H. Suzuki, N. Mangkorntong, and H. Takagi, Physica C **341-348**, 2177 (2000).

[11] T. Jacobs, B.A. Willemsen, S. Sridhar, R. Nagarajan, L.C. Gupta, Z. Hossain, C. Mazumdar, P.C. Canfield, and B.K. Cho, Phys. Rev. B **52**, R7022 (1995).

[12] In-Sang Yang, M.V. Klein, S.L. Cooper, P.C. Canfield, B.K. Cho, and Sung-Ik Lee, Phys. Rev. B **62**, 1291 (2000).

[13] M. Bullock, J. Zarestky, C. Stassis, A. Goldman, P. Canfield, Z. Honda, G. Shirane, and S.M. Shapiro, Phys. Rev. B **57**, 7916 (1998).

[14] J. Zarestky, C. Stassis, A. Goldman, P. Canfield, G. Shirane, and S. Shapiro, Phys. Rev. B **60**, 11 932 (1999).

[15] S.B. Dugdale, M.A. Alam, I. Wilkinson, R.J. Hughes, I.R. Fisher, P.C. Canfield, T. Jarlborg, and G. Santi, Phys. Rev. Lett. **83**, 4824 (1999).

[16] J.W. Lynn, S. Skanthakumar, Q. Huang, S.K. Sinha, Z. Hossain, L.C. Gupta, R. Nagarajan, and C. Godart, Phys. Rev. B **55**, 6584 (1997); K. Nørgaard, M.R. Eskildsen, N.H. Andersen, J. Jensen,

P. Hedegøgaar, S.N. Klausen, and P.C. Canfield, Phys. Rev. Lett. **84**, 4982 (2000).
[17] J.Y. Rhee, X. Wang, and B.N. Harmon, Phys. Rev. B **51**, 15 585 (1995).
[18] C.A. Balseiro and L.M. Falicov, Phys. Rev. B **20**, 4457 (1979).
[19] A.H. Castro Neto, Phys. Rev. Lett. **86**, 4382 (2001).
[20] W.L. McMillan and J.M. Rowell, in *Superconductivity*, edited by R.D. Parks (Marcel Dekker Inc., New York, 1969).
[21] H. Suderow, P. Martinez-Samper, S. Vieira, N. Luchier, J.P. Brison, and P. Canfield, Phys. Rev. B **64**, 020503(R) (2001).
[22] H. Suderow, M. Crespo, P. Martinez-Samper, J.G. Rodrigo, G. Rubio-Bollinger, S. Vieira, N. Luchier, J.P. Brison, and P.C. Canfield, Physica C **369**, 106 (2002).
[23] T. Ekino, H. Fujii, M. Kosugi, Y. Zenitani, and J. Akimitsu, Phys. Rev. B **53**, 5640 (1996).
[24] Y. De Wilde, M. Iavarone, U. Welp, V. Metlushko, A.E. Koshelev, I. Aranson, G.W. Crabtree, and P.C. Canfield, Phys. Rev. Lett. **78**, 4273 (1997).
[25] H. Sakata, M. Oosawa, K. Matsuba, N. Nishida, H. Takeya, and K. Hirata, Phys. Rev. Lett. **84**, 1583 (2000).
[26] J.P. Carbotte, Rev. Mod. Phys. **62**, 1027 (1990).
[27] H. Suderow, E. Bascones, A. Izquierdo, F. Guinea, and S. Vieira, Phys. Rev. B **65**, 100519(R) (2002).
[28] J.G. Rodrigo, N. Agrait, C. Sirvent, and S. Vieira, Phys. Rev. B **50**, 7177 (1994).
[29] S. Manalo, H. Michor, M. El-Hagary, G. Hilscher, and E. Schachinger, Phys. Rev. B **63**, 104508 (2001).
[30] H. Michor, T. Holubar, C. Dusek, and G. Hilscher, Phys. Rev. B **52**, 16 165 (1995).
[31] M. El-Hagary, H. Michor, and G. Hilscher, Phys. Rev. B **61**, 11 695 (2000).
[32] S.V. Shulga, S.-L. Drechsler, G. Fuchs, K.-H. Muller, K. Winzer, M. Heinecke, and K. Krug, Phys. Rev. Lett. **80**, 1730 (1998).
[33] C.J. Chen, *Introduction to Scanning Tunneling Microscopy* (Oxford University Press, New York, 1993).
[34] H.F. Hess, R.B. Robinson, and J.V. Waszczak, Phys. Rev. Lett. **64**, 2711 (1990).
[35] N. Hayashi, M. Ichioka, and K. Machida, Phys. Rev. B **56**, 9052 (1997).
[36] J.M. Daams and J.P. Carbotte, J. Low Temp. Phys. **43**, 263 (1981).
[37] A.A. Golubov and I.I. Mazin, Phys. Rev. B **55**, 15 146 (1997).
[38] E. Bascones and F. Guinea, Phys. Rev. B **64**, 214508 (2001); (private communication).
[39] S.H. Pan, E.W. Hudson, and J.C. Davis, Appl. Phys. Lett. **73**, 2992 (1998).
[40] L.S. Borkowski and P.J. Hirschfeld, Phys. Rev. B **49**, 15 404 (1994).
[41] R. Fehrenbacher and M.R. Norman, Phys. Rev. B **50**, 3495 (1994).
[42] K.O. Cheon, I.R. Fisher, V.G. Kogan, P.C. Canfield, P. Miranovic, and P.L. Gammel, Phys. Rev. B **58**, 6463 (1998).
[43] P.L. Gammel, D.J. Bishop, M.R. Eskildsen, K. Mortensen, N.H. Andsersen, I.R. Fisher, K.O. Cheon, P.C. Canfield, and V.G. Kogan, Phys. Rev. Lett. **82**, 4082 (1999).